JACS
JOURNAL OF THE AMERICAN CHEMICAL SOCIETY

COMMUNICATION

pubs.acs.org/JACS

Thallium Chalcohalides for X-ray and γ-ray Detection

Simon Johnsen,[†] Zhifu Liu,[‡] John A. Peters,[‡] Jung-Hwan Song,[§] Sandy Nguyen,[†] Christos D. Malliakas,[†] Hosub Jin,[§] Arthur J. Freeman,[*,§] Bruce W. Wessels,[*,‡] and Mercouri G. Kanatzidis[*,†]

[†]Department of Chemistry, [‡]Materials Research Center, Department of Materials Science and Engineering, and [§]Department of Physics and Astronomy, Northwestern University, Evanston, Illinois 60208, United States

Supporting Information

ABSTRACT: We report that the chalcohalide compound Tl_6SeI_4 is a promising material for efficient X-ray and γ-ray detection. This material has a higher figure of merit than the current state-of-the-art material for room-temperature operation, $Cd_{0.9}Zn_{0.1}Te$ (CZT). We have synthesized high-quality single-crystalline wafers of Tl_6SeI_4 with detector-grade resistivities and good carrier transport of both electrons and holes. We demonstrate that pulse height spectra recorded using Co-57 radiation show an energy resolution matching that of a commercial CZT detector material.

Semiconducting X- and γ-ray detectors play critical roles in biomedical imaging, spectroscopic instrumentation, national security applications, and several other scientific applications. Currently $Cd_{0.9}Zn_{0.1}Te$ (CZT) is the material of choice for room-temperature operation;[1−4] however, despite decades long development, synthesis of detector-grade CZT remains challenging.[3,5−7] Macro-scale defects such as grains, cracks, and naturally occurring Te precipitates, as well as low intrinsic hole mobility, give limited energy resolution.[3,5−7] New materials are in demand that can detect at room temperature with high signal-to-noise ratio and at low cost.[2,8,9] Materials for X- and γ-ray detectors are highly dense, wide band gap semiconductors (>1.6 eV) with high average Z to ensure high absorption, high electrical resistivity, and high mobility−lifetime products ($\mu\tau$) of the charge carriers.[1−4] The latter quantity can be regarded as a figure of merit for the assessment of detector materials. For these reasons, heavy metal halides such as HgI_2,[10−12] TlBr and $TlBr_{1-x}I_x$,[1,13−15] PbI_2,[16,17] and BiI_3[18] are being intensely investigated as X- and γ-ray detector materials. The halides are all particularly soft, which is problematic because mechanical deformation during wafer fabrication induces structural defects by local plastic deformation and creation of dislocations.[8,14,15] Furthermore, their $\mu\tau$ products are generally smaller than for CZT.

Ideal materials with superior X- and γ-ray detector properties for room-temperature operation require a combination of contraindicated properties in a single compound. For example, metal chalcogenide compounds with heavy elements can have high densities and semiconducting properties but invariably exhibit low band gaps, which lead to large dark currents and render them unsuitable for γ-ray signal detection. The desired density is >6 g/cm^3, and the band gap should range from 1.6 to ∼2.5 eV. The challenge in designing superior γ-ray detectors is to identify heavy element semiconductors with large band gaps. Although this is possible with some halides, e.g., the iodides HgI_2, PbI_2, etc., in general halides have narrow band widths and band gaps that are too large (E_g > 2.6 eV), and consequently photoexcited carriers have low mobilities. The halides are also moisture sensitive. Metal chalcogenides, on the other hand, are robust and can have larger carrier mobilities than halides.

Here we present a novel approach for identifying promising new X- and γ-ray detector materials. The band gaps of the chalcogenides can be widened by merging the features of chalcogenide and halide lattices to consider hybrid chalcohalide compounds. This intuitive phenomenon is well known in chalcohalide noncrystalline cluster chemistry and glass research; however, it is much less studied for extended crystalline materials.[19,20] Chalcohalide hybrids produce a semiconductor structure with a widening of the energy gap toward the desired range. The incorporation of MX_n (M = heavy metal, X = halogen) into binary networks such as M_nQ_m (Q = chalcogen) can create frameworks that are different from those of MX_n or M_nQ_m. In essence, the new ternary lattice formed must accommodate Q and X atoms in an ordered arrangement. The introduction of halide disrupts the extensive orbital overlap of the heavy chalcogenide atoms in the structure and narrows the band widths, creating band gaps that are intermediate between those of pure chalcogenides (too low) and pure halides (too large) (see Figure 1). For example, when the end member TlI ($E_g \approx 2.75$ eV) is mixed with the other end member Tl_2Se ($E_g \approx 0.6$ eV), the resulting ternary chalcogenide/halide compound Tl_6SeI_4 has a very high density and desirable band gap of 1.86 eV.

On the basis of the above line of thought, we propose the class of thallium chalcohalides, e.g., Tl_6SeI_4, as wide gap semiconductors and excellent candidates for X- and γ-ray detection. For example, energy band gaps are in the appropriate range for X- and γ-ray detection,[2,4,9] the structures are dense with a high average Z, and melting points are relatively low, which facilitates crystal growth.[21,22] Tl_6SeI_4, for which synthesis, structure, and thermophysical data have been reported previously,[21,22] melts at 437 °C[22] and crystallizes in a dense (7.38 g/cm^3) tetragonal structure ($P4/mnc$ space group with $a = b = 9.178$ Å and $c = 9.675$ Å).[21] Tl_6SeI_4 has a three-dimensional structure (Figure 2a), which leads to better intrinsic electronic and mechanical properties compared to layered (2D) or linear (1D) compounds.

The attenuation length as a function of impinging photon energy can be calculated using the atomic attenuation coefficients tabulated by NIST.[23] In the entire photon energy range, the calculated attenuation coefficient of Tl_6SeI_4 is larger than that of CZT (see Supporting Information (SI)). Notably, for

Received: April 8, 2011
Published: June 15, 2011

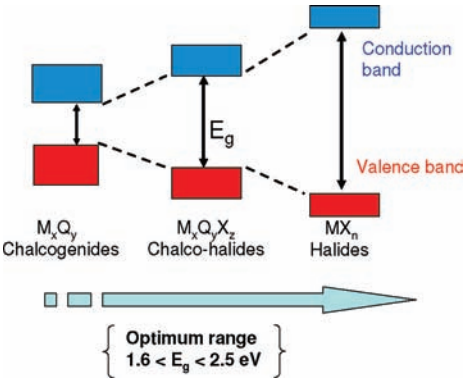

Figure 1. Metal chalcohalide semiconductors materials can have energy gaps that lie between those of the corresponding end member binary chalcogenides and binary halides.

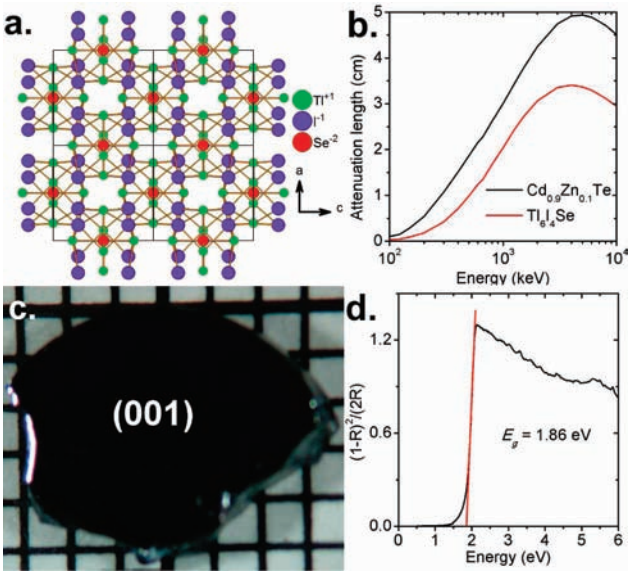

Figure 2. (a) Four unit cells of Tl_6SeI_4 viewed along the *b*-axis. (b) Calculated attenuation length for CZT and Tl_6SeI_4 as a function of incident photon energy. (c) Single-crystalline (001) wafer of Tl_6SeI_4 with dimensions ~4 × ~6 × 2 mm, shown on graph paper with millimeter spacing. (d) Electronic absorption spectrum obtained from diffuse reflectance measurement on ground Tl_6SeI_4 crystals.

high-energy γ-rays the stopping power and absorption coefficients of Tl_6SeI_4 are much greater than those of CZT (Figure 2b). For example, for Co-57 γ radiation at 122 keV (and Cs-137 662 keV radiation in parentheses), the attenuation length in CZT is 1.5 mm (2.3 cm) but only 0.4 mm (1.3 cm) in Tl_6SeI_4. The higher absorption implies that the requirements on the $\mu\tau$ products are less severe and smaller detector dimensions may be used.

Tl_6SeI_4 is the first chalcohalide to be investigated as a semiconducting X- and γ-ray detection material. We succeeded in growing crystals and fabricating high-quality single-crystalline wafers of Tl_6SeI_4 with dimensions suitable for X- and γ-ray detection (Figure 2c). We show that Tl_6SeI_4 exhibits excellent detector material properties, including a band gap in the appropriate range, a high electrical resistivity, and a high $\mu\tau$ product for electrons as well as holes. This is corroborated by detailed band

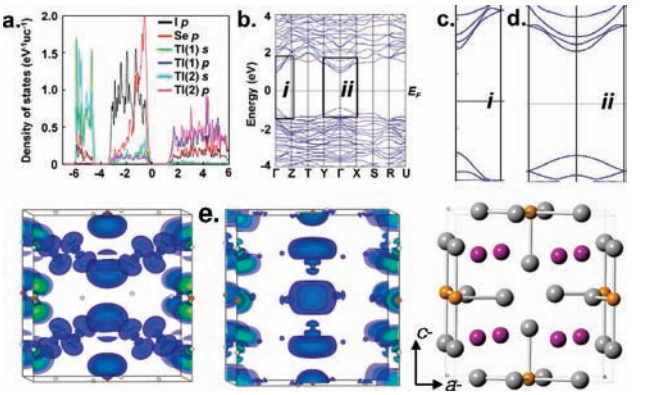

Figure 3. (a) Orbital contributions to the density of states (in units of eV per unit cell) of the crystallographically distinct elements. (b) Band structure of Tl_6SeI_4 calculated using sx-LDA. (c) Zoom-in of excerpt ***i*** in panel b. (d) Zoom-in of excerpt ***ii*** in panel b. (e) Isosurface plots of the charge density near the valence band maximum (VBM, −0.1 eV) and the conduction band minimum (CBM, ~0.1 eV) and their corresponding crystal structure. The orange, gray, and purple spheres are Se, Tl, and I atoms, respectively.

structure calculations, which show that Tl_6SeI_4 is a wide band gap semiconductor with highly dispersed valence and conduction bands. The excellent electron and hole transport in this compound yields a response with resolution matching that obtained with CZT but with a significantly smaller amount of tailing.

Crystals of Tl_6SeI_4 were grown using a modified vertical Bridgman technique in a dual-zone furnace. The resulting sample shows single-crystalline domains from which wafers were cut perpendicular to the growth direction, which was determined to be the ⟨001⟩ direction by Laue X-ray back reflection. Figure 2c shows a polished (001) wafer. Though Tl_6SeI_4 has to be handled with care because of the toxicity of thallium, the mechanical properties of the Tl_6SeI_4 phase are good, and cutting and polishing were readily done without breaking or deforming the crystals. Overall, the crystals appear black but are transparent red in transmitted light, in agreement with the band gap of 1.86 eV (Figure 2d). This is in the optimum band gap range for X- and γ-ray detector materials[1,2,4,9] because it is wide enough to avoid thermally generated carriers yet sufficiently narrow to generate a significant number of carriers, as the pair creation energy is usually given by ~$3E_g$.[24]

The experimental band gap (1.86 eV) is in excellent agreement with the screened exchange local-density approximation electronic band structure calculations for Tl_6SeI_4, which show a direct band gap of 1.89 eV at the Γ point. In the thallium halides the band gap is indirect, with disperse conduction and valence bands.[25,26] The incorporation of Se changes the nature of the gap from indirect to direct and results in a marked narrowing of the band gap from 2.75 eV in the case of TlI[27] to 1.89 eV in Tl_6SeI_4. Both conduction and valence bands show large dispersion near the band edges, especially for the direction along Γ to *Z* (Figure 3c,d). The anisotropy between the in-plane (Γ to X or Y) and the out-of-plane (Γ to *Z*) also can be seen in the isosurface plots (Figure 3e) of the charge density near the band edges; the octahedral units of Se with Tl neighbors make significant contribution to the band edges; however, the contribution of the in-plane Tl atoms (Tl(2) in Figure 3a) is negligible compared to that of the out-of-plane ones (Tl(1) in Figure 3a). This anisotropy can be accounted for by crystal packing, due to the

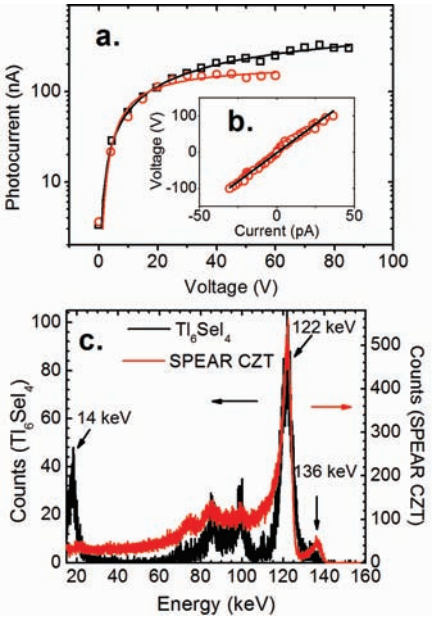

Figure 4. (a) Photocurrent versus applied voltage from electrons and holes measured on a ~6 × 4 × 2 mm Tl_6SeI4 (001) wafer along ⟨001⟩. (b) Current−voltage characteristics of a ~6 × 4 × 2 mm Tl_6SeI_4 (001) wafer measured along ⟨001⟩. (c) Recorded pulse height spectrum from γ radiation from a Co-57 source using a 6 × 4 × 2 mm (001) Tl_6SeI_4 wafer (red solid line) and a commercial 5 × 5 × 5 mm SPEAR CZT detector. Measurements were carried out at 295 K.

longer distance (3.08 Å) of the Se−Tl bond along the in-plane than that (2.96 Å) along the out-of-plane. The in-plane Tl atoms have relatively stronger hybridization with I atoms that contributes to more localized and deeper energy states compared to the out-of-plane Tl atoms (Figure 3a). This makes the contribution to the band edges small along the in-plane direction (Figure 3e). To see more clearly the effect of the anisotropy near the band edges, we have evaluated the effective masses, which yield 0.18 m_0 (m^*_{zz}) and 0.91 m_0 (m^*_{xx}) for holes, and 0.15 m_0 (m^*_{zz}) and 0.46 m_0 (m^*_{xx}) for electrons. In CdTe the corresponding effective masses are 0.11 m_0 for electrons and 0.73 m_0 for holes.[3] Since the mobility is inversely proportional with the effective mass, high hole $\mu\tau$ products are not feasible in CZT. According to the band structure calculations, Tl_6SeI_4 has no such intrinsic barrier to high $\mu\tau$ products for electrons or holes, and furthermore the calculations suggest that wafers with transport along ⟨001⟩ are best suited for detection purposes. Furthermore, the considerable cross-band hybridization observed above can lead to a high static dielectric constant that effectively screens charged defects and impurities, as has recently been observed for TlBr, which has high $\mu\tau$.[28] In order to elucidate this point, detailed optical properties measurements are underway.

The experimental $\mu\tau$ values for both carrier types can be estimated by fitting the photocurrent response under negative and positive bias voltages to Many's equation.[29] This analysis shows high mobility−lifetime products: $\mu\tau_h = 6 \times 10^{-4}$ cm^2·V^{-1} for holes and $\mu\tau_e = 7 \times 10^{-3}$ cm^2·V^{-1} for electrons. In comparison, the corresponding values for optimized Bridgman-grown CZT (commercially available from eV Products)[30] are $\mu\tau_h \approx (0.5-5) \times 10^{-5}$ cm^2·V^{-1} and $\mu\tau_e = (3-11) \times 10^{-3}$ cm^2·V^{-1}. Further improvements of $\mu\tau$ values are expected in the future as has been possible previously with currently available materials. For example, since CZT and TlBr were first considered for detector applications, continued development produced an increase in their $\mu\tau$ products respectively by 1 and 3 orders of magnitude.[13,14] Since photon absorption at high incident energies is substantially higher in Tl_6SeI_4 than in CZT (~3 times at 122 keV), superior resolution and performance can be expected in the thinner Tl_6SeI_4 detectors.

In addition to high $\mu\tau$ values, efficient detector materials have high resistivities to minimize dark currents. Current−voltage behavior for a (001) wafer cut perpendicular to the growth direction is shown in Figure 4b. The very high resistivity of the Tl_6SeI_4 wafer caused the measurement signal to approach the impedance limit of our instrument, giving a resistivity of ~4 × 10^{12} Ω·cm along ⟨001⟩. This is several orders of magnitude above the general requirement of >10^8−10^9 Ω·cm for detector-grade materials,[3,9] and superior to detector-grade CZT, which has resistivity typically of the order 10^{10}−10^{11} Ω·cm.[1,3,9,31,32] This implies lower leakage currents in Tl_6SeI_4 and the possibility to use higher electric fields to increase resolution and decrease the readout time.

Mechanical deformation during cutting and handling induces stress and damage in the crystals. Hence, hardness is an important factor for detector materials and fabrication. The measured Knoop hardness (at 10 g load for 10 s) of Tl_6SeI_4 is 72 ± 2 kg·mm^{-2}, making it comparable to CdTe and ZnTe (~60 and ~80 kg·mm^{-2})[9,33] and significantly harder than most heavy metal halides (e.g., TlBr has a Knoop hardness of 12 kg·mm^{-2}, similar to that of refrigerated butter).[9,14] The greater hardness of Tl_6SeI_4 suggests an easier future transition from laboratory to commercial applications.

Pulse height spectra were recorded using a Co-57 source which emits 14.4, 122.1, and 136.5 keV radiation with relative intensities of 0.11, 1, and 0.12, respectively (Figure 4). All major peaks are clearly resolved. The energy resolution is 5.7 keV at fwhm for the 122.1 keV, corresponding to 4.7%. For the commercial SPEAR CZT detector, the corresponding value is 5.54 keV (4.5%) at 122.1 keV. Additional peaks are observed at ~85, 99, and 110 keV for the Tl_6SeI_4 wafer. The latter two are attributed to escape peaks owing to I Kα and Se Kα radiation, respectively. They arise from photons knocking out core electrons of the elements, which then emit unabsorbed characteristic X-rays. Consequently, the detector reads a photon minus the characteristic photon energy. The peak at ~85 keV is from photons that are backscattered in the detector and remain unabsorbed. The position of this peak is solely dependent on the incident photon energy, not the composition, and consequently it is also observed in the CZT detector. The remaining two peaks in CZT, at ~74 and ~99 keV, are due to Pb Kα from the lead shielding used during the experiment and a Te Kα escape peak.

Large differences in the electron and hole collection times leads to a low energy tail.[1,4,15] This is the case for CZT and clearly is observed on the 122 keV peak for CZT. For the Tl_6SeI_4 detector, no energy tails are observed, which suggests similar charge collection times for electrons and holes. This is corroborated by the similar $\mu\tau$ values obtained from the photoconductivity measurements. For Tl_6SeI_4 there is an order of magnitude difference in the $\mu\tau$ for electrons and holes, while there is typically at least 2 orders of magnitude difference for CZT. To overcome the poor hole transport and enhance the resolution of CZT detectors, elaborate detector designs and pulse discrimination techniques are used.[4] In the latter, acceptance of only the short pulses from the more mobile electrons gives an enhancement

in resolution at a cost in detector efficiency. Owing to the significantly reduced tailing in the Tl_6SeI_4 detector, it appears no such signal processing nor elaborate detector setups will be necessary to compensate for poor hole transport. Detrimental polarization effects, which are present in most detector materials including CZT,[3,14] have not been investigated in detail for Tl_6SeI_4 but are expected and need future attention. Suitable contact materials and moderate cooling of the detector material have previously been shown to effectively eliminate polarization effects in TlBr.[14,34]

Thallium chalcohalides constitute a promising new class of X- and γ-ray semiconducting detector materials. They combine a set of useful physical properties that is challenging to achieve in a single material, namely highly dense crystal structures, elements with high atomic number (e.g., high Z), and wide energy band gap. Here, we have shown how detector-size and detector-grade Tl_6SeI_4 single crystals can be prepared with a higher figure of merit than CZT. Unlike many detector materials, which suffer from poor hole transport, both carrier types are highly mobile in Tl_6SeI_4. This results in pulse height spectra with no tailing, which could increase resolution and simplify detector design. Significant increases in detector performance, similar to the historical improvement of the legacy materials TlBr and CZT, can be expected for Tl_6SeI_4 with continued improvements in crystal growth, wafer fabrication, and device processing. Consequently, not only Tl_6SeI_4 but also related compounds have the potential to emerge as new, efficient semiconducting X- and γ-ray detector materials with properties superseding CZT.

■ ASSOCIATED CONTENT

Supporting Information. Experimental details; Figure S1, calculated attenuation length as a function of incident photon energy in Tl_6SeI_4 and CZT for a wider incident photon energy scale; Figure S2, temperature profile of the dual-zone furnace used in crystal growth; Figure S3, as-synthesized Tl_6SeI_4 sample before waferizing; Figure S4, X-ray Laue back-reflection and refined simulated pattern for (001) wafer; Figure S5, X-ray powder diffraction pattern of ground Tl_6SeI_4; Figure S6, Knoop hardness indents and details of the Knoop hardness calculations; Figure S7, schematic of the setup used to collect pulse height spectra. This material is available free of charge via the Internet at http://pubs.acs.org.

■ AUTHOR INFORMATION

Corresponding Author
m-kanatzidis@northwestern.edu

■ ACKNOWLEDGMENT

S.J. acknowledges funding from the Danish Research Council for Nature and Universe. This work is supported in part by the Department of Homeland Security with grant 2010-DN-077-ARI042-02 and in part by a Defense Threat Reduction Agency grant HDTRA1 09-1-0044. Device fabrication was performed in the microfabrication facility of the Materials Research Center at Northwestern University supported by the NSF under grant DMR-0076097.

■ REFERENCES

(1) Owens, A. *J. Synchrotron Radiat.* **2006**, *13*, 143.
(2) Milbrath, B. D.; Peurrung, A. J.; Bliss, M.; Weber, W. J. *J. Mater. Res.* **2008**, *23*, 2561.
(3) Schlesinger, T. E.; Toney, J. E.; Yoon, H.; Lee, E. Y.; Brunett, B. A.; Franks, L.; James, R. B. *Mater. Sci. Eng.: Reports* **2001**, *32*, 103.
(4) McGregor, D. S.; Hermon, H. *Nucl. Instrum. Methods Phys. Res., Sect. A* **1997**, *395*, 101.
(5) Amman, M.; Lee, J. S.; Luke, P. N. *J. Appl. Phys.* **2002**, *92*, 3198.
(6) Bolotnikov, A. E.; Camarda, G. S.; Carini, G. A.; Cui, Y.; Li, L.; James, R. B. *Nucl. Instrum. Methods Phys. Res., Sect. A* **2007**, *571*, 687.
(7) Szeles, C. *Phys. Stat. Solidi B: Basic Res.* **2004**, *241*, 783.
(8) Owens, A.; Bavdaz, M.; Lisjutin, I.; Peacock, A.; Sipila, H.; Zatoloka, S. *Nucl. Instrum. Methods Phys. Res., Sect. A* **2001**, *458*, 413.
(9) Owens, A.; Peacock, A. *Nucl. Instrum. Methods Phys. Res., Sect. A* **2004**, *531*, 18.
(10) Swierkowski, S. P.; Armantrout, G. A.; Wichner, R. *IEEE Trans. Nucl. Sci.* **1974**, *21*, 302.
(11) Owens, A.; Bavdaz, M.; Brammertz, G.; Krumrey, M.; Martin, D.; Peacock, A.; Troger, L. *Nucl. Instrum. Methods Phys. Res., Sect. A* **2002**, *479*, 535.
(12) van den Berg, L.; Vigil, R. D. *Nucl. Instrum. Methods Phys. Res., Sect. A* **2001**, *458*, 148.
(13) Shah, K. S.; Lund, J. C.; Olschner, F.; Moy, L.; Squillante, M. R. *IEEE Trans. Nucl. Sci.* **1989**, *36*, 199.
(14) Churilov, A. V.; Ciampi, G.; Kim, H.; Higgins, W. M.; Cirignano, L. J.; Olschner, F.; Biteman, V.; Minchello, M.; Shah, K. S. *J. Cryst. Growth* **2010**, *312*, 1221.
(15) Owens, A.; Bavdaz, M.; Brammertz, G.; Gostilo, V.; Graafsma, H.; Kozorezov, A.; Krumrey, M.; Lisjutin, I.; Peacock, A.; Puig, A.; Sipila, H.; Zatoloka, S. *Nucl. Instrum. Methods Phys. Res., Sect. A* **2003**, *497*, 370.
(16) Shah, K. S.; Bennett, P.; Klugerman, M.; Moy, L.; Cirignano, L.; Dmitriyev, Y.; Squillante, M. R.; Olschner, F.; Moses, W. W. *IEEE Trans. Nucl. Sci.* **1997**, *44*, 448.
(17) Deich, V.; Roth, M. *Nucl. Instrum. Methods Phys. Res., Sect. A* **1996**, *380*, 169.
(18) Matsumoto, M.; Hitomi, K.; Shoji, T.; Hiratate, Y. *IEEE Trans. Nucl. Sci.* **2002**, *49*, 2517.
(19) Wang, L.; Hung, Y. C.; Hwu, S. J.; Koo, H. J.; Whangbo, M. H. *Chem. Mater.* **2006**, *18*, 1219.
(20) Wang, L.; Hwu, S. J. *Chem. Mater.* **2007**, *19*, 6212.
(21) Blachnik, R.; Dreisbach, H. A.; Pelzl, J. *Mater. Res. Bull.* **1984**, *19*, 599.
(22) Peresh, E. Y.; Lazarev, V. B.; Korniichuk, O. I.; Tsigika, V. V.; Petrushova, O. V.; Kish, Z. Z.; Semrad, E. E. *Inorg. Mater.* **1993**, *29*, 440.
(23) Seltzer, S. M. *Radiat. Res.* **1993**, *136*, 147.
(24) Alig, R. C.; Bloom, S. *Phys. Rev. Lett.* **1975**, *35*, 1522.
(25) Schreiber, M.; Schafer, W. *Phys. Rev. B* **1984**, *29*, 2246.
(26) Kolinko, M. I.; Kityk, I. V.; Krochuk, A. S. *J. Phys. Chem. Solids* **1992**, *53*, 1315.
(27) Samara, G. A.; Walters, L. C.; Northrop, D. A. *J. Phys. Chem. Solids* **1967**, *28*, 1875.
(28) Du, M. H.; Singh, D. J. *Phys. Rev. B* **2010**, 81.
(29) Many, A. *J. Phys. Chem. Solids* **1965**, *26*, 575.
(30) Bale, D. S.; Szeles, C. *J. Electron. Mater.* **2009**, *38*, 126.
(31) Chen, H.; Awadalla, S. A.; Mackenzie, J.; Redden, R.; Bindley, G.; Bolotnikov, A. E.; Camarda, G. S.; Carini, G. *IEEE Trans. Nucl. Sci.* **2007**, *54*, 811.
(32) Awadalla, S. A.; Mackenzie, J.; Chen, H.; Redden, B.; Bindley, G.; Duff, M. C.; Burger, A.; Groza, M.; Buliga, V.; Bradley, J. P.; Dai, Z. R.; Teslich, N.; Black, D. R. *J. Cryst. Growth* **2010**, *312*, 507.
(33) Adachi, S. *Properties of Group-IV, III-V and II-VI Semiconductors*; Wiley: Chichester, 2005.
(34) Hitomi, K.; Shoji, T.; Nlizeki, Y. *Nucl. Instrum. Methods Phys. Res., Sect. A* **2008**, *585*, 102.